PROCEEDINGS OF SCIENCE

# Carbon based local supports for the ATLAS ITk-pixel detector

**F. J. Munoz*** **and on behalf of the ATLAS ITk pixel collaboration**

*University of Manchester,*
*Department of Physics and Astronomy,*
*Oxford Road, Manchester,*
*M13 9PL, UK*

*E-mail:* fmunoz@cern.ch

The current ATLAS Inner Detector will be upgraded to the Inner Tracker detector for its operation at the High Luminosity Large Hadron Collider. The Inner Tracker will be an all-silicon detector divided into two sub-detectors: four layers of strip sensors will form the strip detector, and five barrel and a number of endcap layers of pixel sensors will form the pixel detector. Local support structures will mechanically support the silicon modules and some of the services including cooling pipes. Specialised carbon-based structures have been designed to optimise performance and provide hermetic coverage. The design of these structures, as well as their thermal, mechanical, and electrical properties, have been qualified by direct tests on prototypes. In this document, the novel designs, assembly procedures, and qualification techniques used to prove their adherence to specifications will be discussed together with the obtained results. Finally, plans for production, expected to start in mid 2023, will also be introduced.

*12-16 December 2022*
*Santa Fe, New Mexico, USA*

*Speaker





PoS(Pixel2022)077

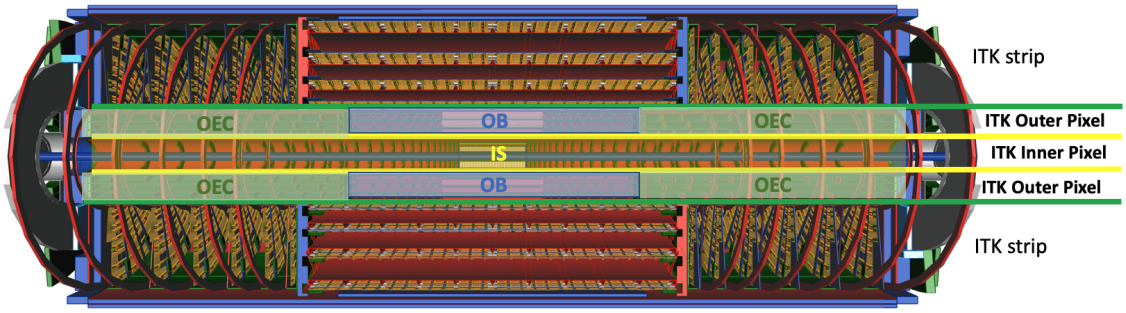


**Figure 1:** A modified ATLAS ITk layout is shown [4] where the different sub-detectors forming the pixel sub-system have been highlighted. The Inner System (IS) in yellow, the Outer Barrel (OB) in blue and two Outer Endcaps (OECs) in green.

## 1. Introduction

The upgrade of the Large Hadron Collider (LHC) to the High Luminosity LHC (HL-LHC) will increase peak and integrated luminosities by factors of 7.5 and 13 respectively [1]. The HL-LHC is designed to deliver radiation fluence values up to $1 \times 10^{16} n_{eq}/cm^2$ in the tracking volume occupied by the current Inner Detector, reaching pile-up mean value of 200 events. The Inner Detector was not designed to operate under such conditions and therefore it will be upgraded to an all-silicon tracker: the ATLAS Inner Tracker (ITk). The ATLAS ITk consists of five layers of strip sensors forming the strip detector [2] in the outermost layers, and five barrel layers plus several endcaps layers of pixel sensors, making the pixel detector [3] closer to the interaction point. In figure 1, the layout of the ITk is shown where the three different subsystems of the pixel detector have been highlighted.

In the ITk Pixel detector there will be different silicon sensors technologies. 150$\mu$m-thick planar sensors will be used in the outer system (OB+OEC), while in the Inner System thinner (100$\mu$m-thick) planar sensors are used on the outermost layer and 3D sensors are used in the innermost layer.

For the best performance of the silicon modules and to avoid thermal runaway, the silicon sensors need to be kept at low temperatures. ATLAS-ITk will be cooled down to -35°C using a $CO_2$ bi-phase cooling system driven through titanium pipes as close as possible to the modules.

### 1.1 ITk Pixel detector

Figure 2 shows a quadrant of the ITk Pixel detector, highlighting the positions of the silicon sensors in the three different sub-systems. The Local Support (LS) structures of each sub-system have been designed not only to support modules and services but also to cool them as efficiently as possible.

In this work, the different pixel local support designs will be described, as well as the assembly procedures. Some of the qualification techniques used and results that prove their adherence to specifications will be discussed. Finally, an overview of the path towards production will be given.

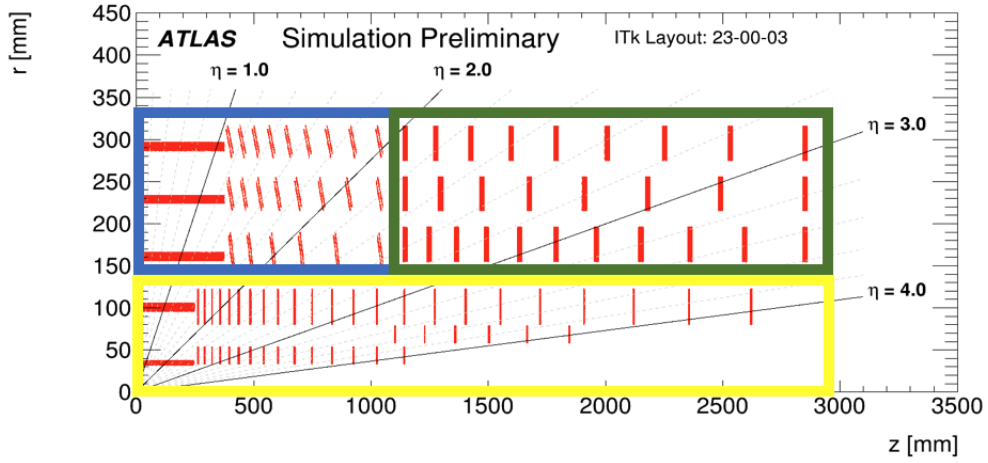


**Figure 2:** A quadrant of the ITk pixel detector is shown (modified from [4]) where the silicon active sensors are shown (in red) and the different pixel sub-systems are indicated by different colours (IS-yellow, OB-blue, OEC-green).

## 2. Pixel local support designs

The three ITk Pixel detector sub-systems have chosen to make their local supports of carbon based materials. Particularly, carbon-fiber-reinforced polymers (CFRP) have a low coefficient of thermal expansion, provide good tensile properties, have high thermal and electrical conductivity and are strong and light materials. Carbon-based structures provide reliable support for the pixel modules and a low thermal-impedance path between the coolant and the module while providing a low total radiation length. In this section an overview of the three sub-systems' local supports is given.

### 2.1 Outer Barrel (OB)

The OB local supports are based on a modular strategy. The OB approach consists of fabricating independent module cells that are screwed onto a framework at a late stage of the production and are therefore independently replaceable. This system provides absolute re-workability, but at the cost of additional production steps during sub-system integration.

The OB module-cell design is shown in figure 3-left. The pixel module is glued onto a pyrolytic graphite tile, which itself has already been glued to a cooling block; this assembly is then screwed onto a base block. The base block has been previously soldered in the desired position along the local support via the cooling pipe (previously attached to the LS). The cooling pipes are part of the main carbon structure of the local supports, which can be an Inclined Half-ring or a Longeron, see figure 3-right. Inclined Half-rings are grouped in Inclined Sections that are then joined together by longerons.

### 2.2 Outer Endcaps (OEC)

The Outer Endcaps consist of three concentric cylinders that mechanically support the Half-rings, see figure 4. The OEC Half-rings will be made in three different sizes, but they will have

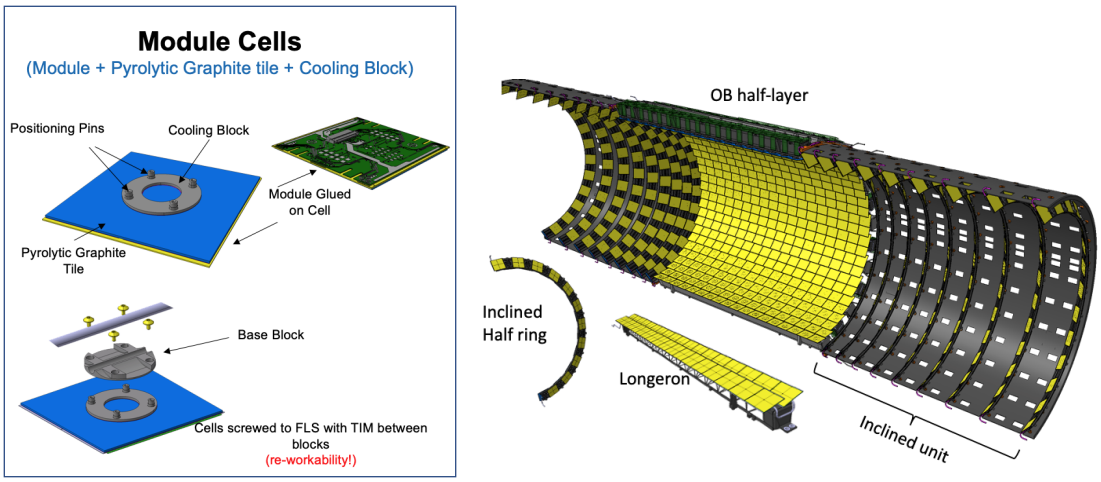


**Figure 3:** Left: Outer Barrel module cell exploded view. Right: Outer Barrel local supports (Inclined Half-Ring and Longeron) designs and a fully-assembled half layer made out of two Inclined Sections and Longerons.

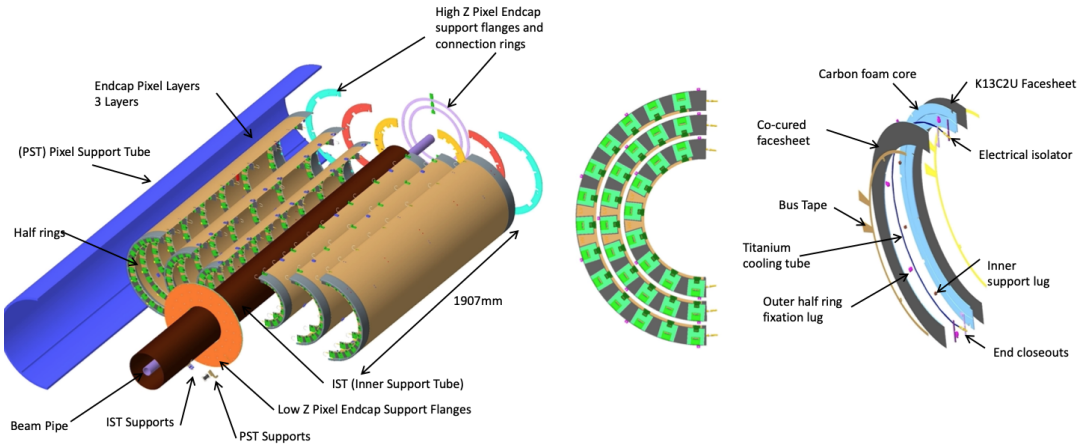


**Figure 4:** Left: full layout of one Outer Endcap, center: transverse view of one Outer Endcap where the three different Half-ring sizes are visible; right: exploded view of one Half-ring where all the components are visible.

identical structure and composition. The cooling pipe is embedded between two layers of carbon foam co-cured to carbon face-sheets (made from three pre-impregnated carbon fibre layers). The two carbon layers, the pipe and some small plastic parts (closeouts, inserts and mounting lugs) are then glued together making the final local support onto which the modules and local services (bus tape) will be loaded at a later stage on both sides of the half-ring. The module positions on one side of the half-ring correspond to spaces between modules on the other side providing full coverage.

### 2.3 Inner System (IS)

The structure of the Inner System local supports is similar to that of the Outer Endcaps: co-cured carbon fiber to carbon foam layers glued together embedding the cooling pipe. The IS however is supported globally in quarter-shells that have barrel and endcap sections. In the barrel

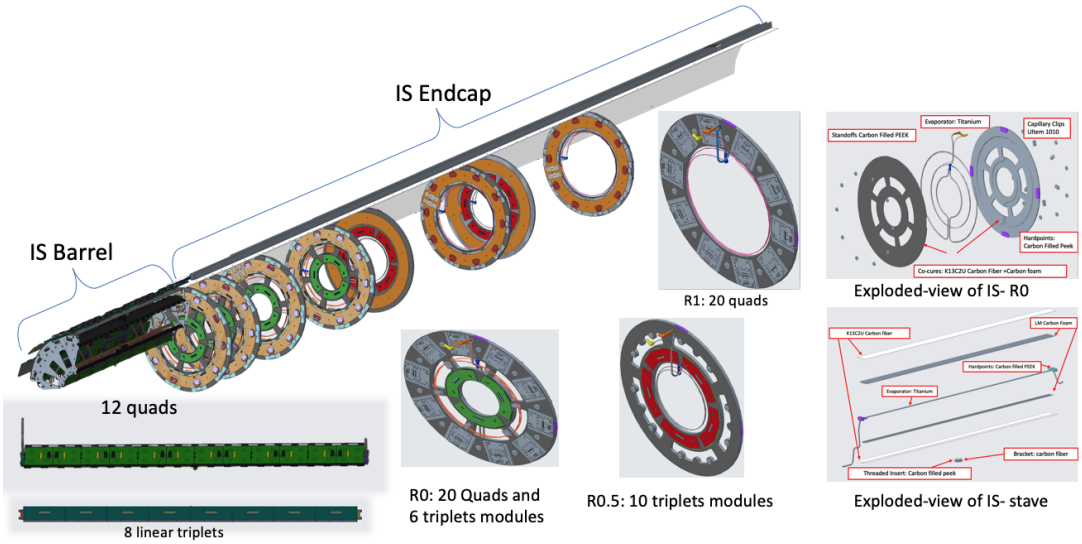


**Figure 5:** The Inner System design. A quarter shell is formed by staves of two different sizes in the central region and the endcap region will consist on several rings of the three different flavours. Some exploded views of the local supports are also shown on the right.

section the local supports will be staves of two different sizes for layers 0 and 1, while in the endcaps there will be three different ring flavours: R0, R0.5 and R1 (see figure 5 for details). The four quarter-shells support rings at different z-positions so there won't be big gaps between rings.

## 3. Local supports design qualification

The local support designs need to be qualified and validated before production can begin. To achieve that, studies based on Finite Element Analysis and measurements on prototypes have been carried out. The materials, interfaces and assemblies to be used in the detector also need to be qualified under the expected conditions in the final detector (e.g. thermal and mechanical stresses, radiation damage).
In this section, only a few examples of this work are shown. The amount, detail and diversity of the studies and measurements carried out by the ATLAS ITk-pixel community in the last ten to twenty years make it impossible to include all of them in a single publication.

### 3.1 Finite Element Analysis

Experts from the three sub-systems worked together to develop parallel and comparable thermal and mechanical models for Finite Element Analysis (FEA) studies. Two different models were required to reflect the structural, material, geometry and assembly differences between systems, they are illustrated in figure reffig:ThermalFEA. In the case of the OEC and the IS, the path between the cooling pipe and the module will consist of the pipe wall, adhesive, carbon foam, CFRP skin and the adhesive between the module and the carbon surface of the LS. In the case of the IS, the path will consist of the pipe wall, the solder to the base block, base block, thermal interface, cooling block and the adhesive to the pyrolytic graphite tile where the modules will be glued.

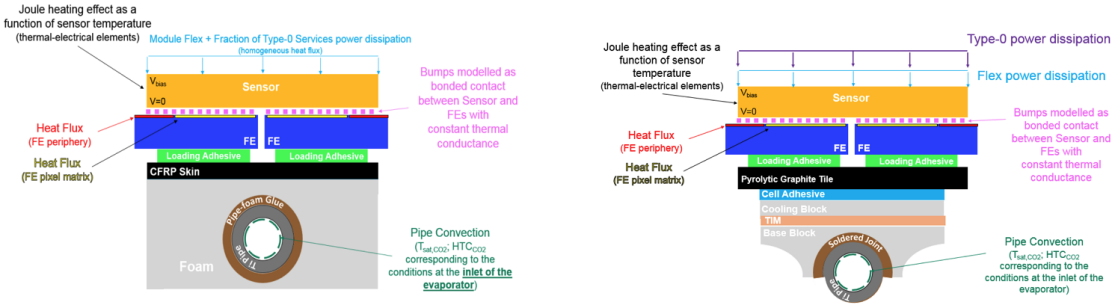


**Figure 6:** Thermal FEA models. Left: Outer Endcap and Inner System model where there will be modules at both sides of the cooling pipe. Right: Outer Barrel model where the different components are visible.

| FE Power dissipation (W/cm²) | | Case 1 | | Case 2 | |
|---|---|---|---|---|---|
| System | Sensors | Matrix | Periphery | Matrix | Periphery |
| Outer (barrel and endcaps) | Planar (150 um) | 0.548 | 0.548 | 0.264 | 3.592 |
| Inner system | Planar (100 um) | 0.8 | 0.8 | 0.30 | 3.75 |
| | 3D sensors | 0.8 | 0.8 | 0.33 | 4.16 |

**Figure 7:** Table summarising the expected front-end chip power dissipation in case of homogeneous distribution (case 1) and during detector operation (case 2).

In terms of commonalities, pipe, coolant and modules were modelled identically in all subsystems, since they will be the same. The only difference between modules to take into account are the different sensor flavours when applicable, see section 1) .

A number of different powering scenarios were considered, two of which will be mentioned here. Case 1 assumes homogeneous power dissipation in the front-end chip (FE); this corresponds to the measurement of the thermal impedance in the laboratories where silicon heaters (homogeneous power dissipation) were loaded before real modules were available. This case was used to validate the different material characteristics used in the model. Case 2 however, corresponds to an improved model that recognises that the power density along the back edge of the FE is 14 times higher than the power density in the pixel matrix. In figure 7 the different power values used for these studies are listed.

The FEA results shown in this document correspond to the expected end of life of the detector, when the heat dissipation will reach its maximum value. The $CO_2$ boiling temperature is -35 $°C$ and the different radiation doses expected in different parts of the detectors were also considered. In figure 8, FEA results of the temperature distribution on the silicon sensors for the three different subsystems are shown.

The thermal impedance between the coolant and the hottest point on the surface of the loaded local support is called the **Thermal Figure of Merit (TFM)** and it is defined as:

$$TFM = \frac{T_{Max} - T_{coolant}}{\frac{Power}{Area}} \tag{1}$$

The power density used to estimate the TFM values takes into account the heat dissipated by the front-end chips, the sensor and the local services, including safety factors. The values of TFM

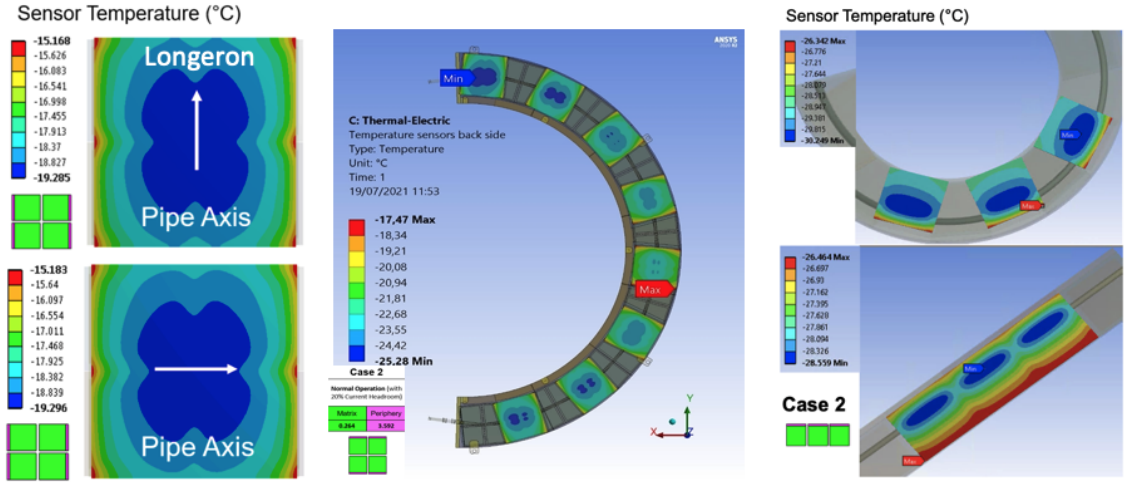


**Figure 8:** Finite Element analysis temperature results for the three subsystems where the maximum temperature expected at the end-of-life of the detector is shown. Left: Outer Barrel Longeron (up), Inclined HR (bottom). Center: Outer Endcap HR. Right: Inner System Ring (up), Stave (bottom).

| [Kcm$^2$/W] | TFM value from FEA | TFM nominal |
|---|---|---|
| Outer Barrel Longeron | 24.34 | 28.85 |
| Outer Barrel IHR | 24.34 | 28.85 |
| Outer Endcap HR | 25.04 | 28.85 |
| Inner System Stave | 12.2 | 13.72 |
| Inner System Ring | 12.3 | 13.72 |

**Table 1:** TFM values in Kcm$^2$/W obtained through FEA calculations compared with the nominal values

obtained by FEA and the nominal values provided by the project specifications are listed in Table 1.

The local supports for the three subsystems have also been mechanically studied both through FEA and with measurements on prototypes. However, the complexity of these studies prevents their inclusion in this document.

### 3.2 Measurements on prototypes

In addition to the calculations through FEA, prototypes were fabricated and the thermal impedance (TFM) was measured using silicon heaters instead of real modules as mentioned above (Case 1). In figure 9 two OB prototypes are shown, an IHR and a Longeron, on which some heaters have been loaded. TFM results are shown, where most of the cells are below the target value and all of them are well below the design value for both local supports, thereby meeting the specifications.

Results for one OEC prototype are shown in figure 10. In this case, the prototype used was known to have assembly defects in two specific areas. Heaters were loaded on the central area (not defective) and some heaters were also placed on the areas with known defects to understand their impact on the thermal impedance and help to define a reliable quality control protocol.

Additionally, the loaded prototype was cycled 100 times in temperature (from -55 $^\circ C$ to +60 $^\circ C$) and pressure (from 0 to 162 bar). The TFM was measured at different stages in between cycles

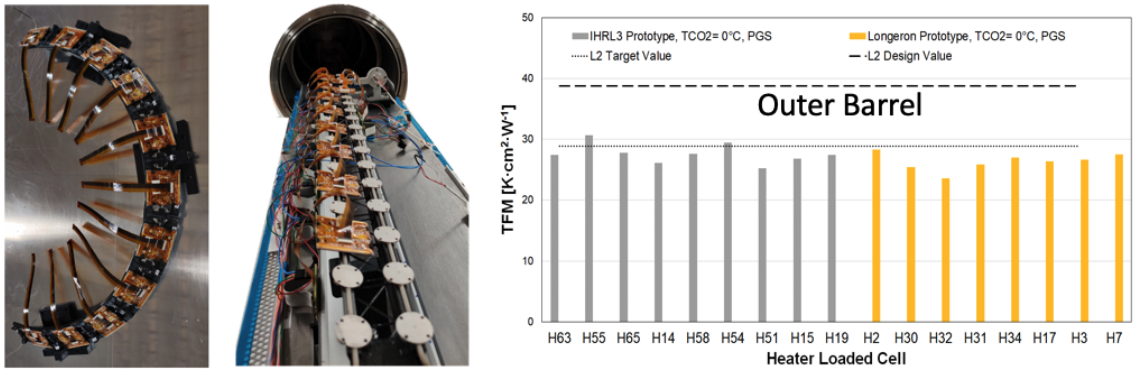


**Figure 9:** Left: IHR populated with silicon heaters. Center: Longeron partially populated with silicon heaters. Right: TFM measurement results for IHR (grey) and Longeron (yellow) prototypes.

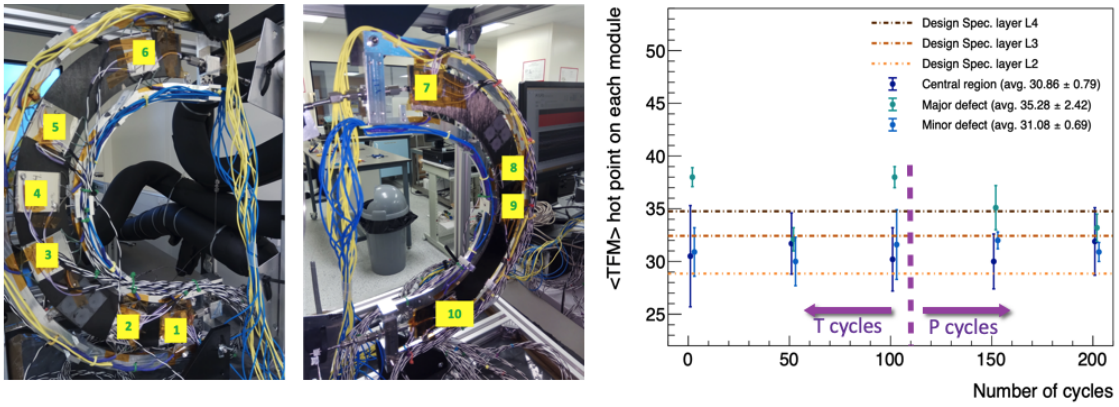


**Figure 10:** Left and center are pictures of a prototype used for design validation on the OEC system. Right: TFM results in three different regions. Non-defective area (dark blue), area with a major defect (green), area with a minor defect (light blue). The design specifications are also indicated.

to allow for identification of any failures that could have occurred while cycling. The results of those measurements show that major assembly defects can impact the thermal performance of the local support as well as that the measured TFM values were not good enough for layer 2 half-rings. Due to these results, the OEC community decided to change the carbon foam for one with higher density and higher thermal conductivity.

In figure 11, TFM results are shown for one of the IS rings where most of the measurements meet specifications; where that's not the case a value slightly over the specification is due to understood problems with the loading of the heaters.

### 3.3 Materials and Assemblies qualification

The HL-LHC will deliver the highest luminosity in a hadron collider up to now, therefore together with the whole assembly, all materials and interfaces between materials need to be qualified to stand the harsh radiation fluences. All subsystems have prepared specific samples and test stands as part of ITk-coordinated irradiation campaigns. The list of materials and tests is very extensive, so in this document only a few results are shown to illustrate the huge effort of the community.

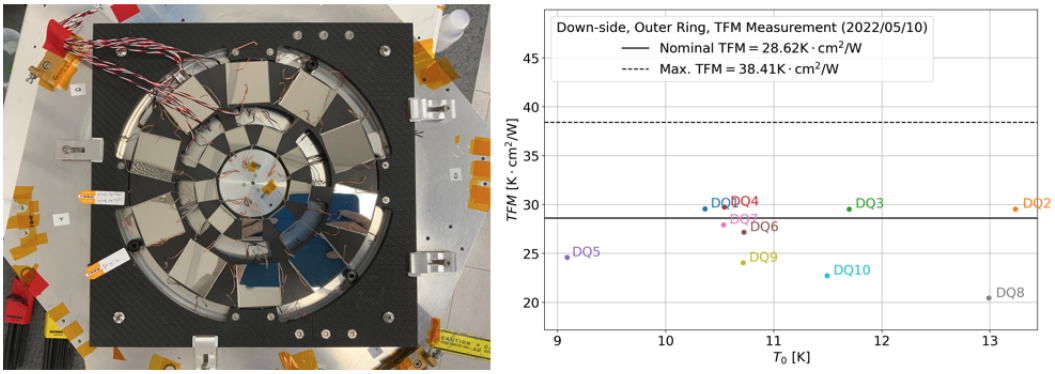


**Figure 11:** Left: picture of an IS ring populated with heaters. Right TFM results ($T_0$ is the $\delta T$ without heat load.

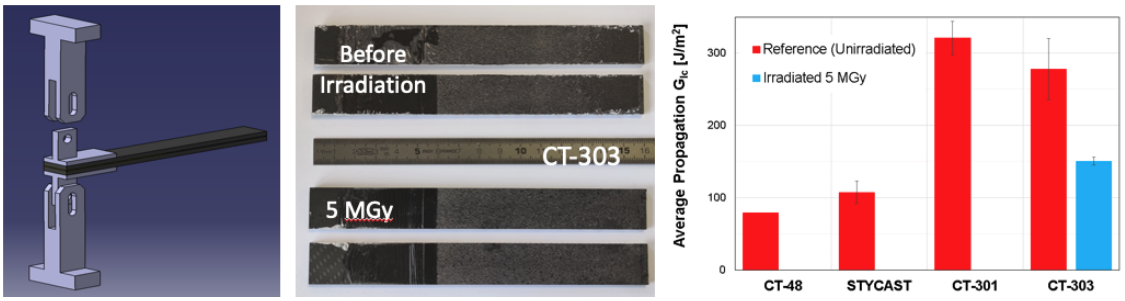


**Figure 12:** Left: sketch of the test and the sample. Center: destroyed samples after the test where glue residuals are left in both sides of the sample. Right: $G_{IC}$ measurement for different adhesive-samples (red) and one adhesive-sample after 5 MGy irradiation.

In figure 12, results of the characterisation of different adhesives are shown, including one (CT-303) irradiated up to 5 MGy. The characterisation is done following the BS ISO 25217:2009 standard both to prepare and to test the Double Cantilever Beam (DCB) samples. In this measurement, the adhesive fracture energy ($G_{IC}$) is measured.

Polymeric materials also needed to be qualified, and "dogbone" samples (three per dose) were made to measure the tensile modulus after the sample has been irradiated up to 15 MGy, see in figure 13. These measurements were compared with historical CERN records [5].

The last result that is shown in this document corresponds to three-point bending tests carried out on OEC local-support-like structures. The sample consists of two layers of co-cured carbon facesheet to carbon foam glued together following the same procedure and adhesive that will be used in the final local supports. With this measurement the apparent flexural stiffness of the samples was measured and no particular trend was found due to irradiation (see figure 14).

## 4. Summary, current status and future steps

This contribution has described the design of the ITk-Pixel local supports and some of the studies carried out by the community to validate the design and qualify the materials.
At the moment of writing this document the outer system (OB + OEC) is half-way through the

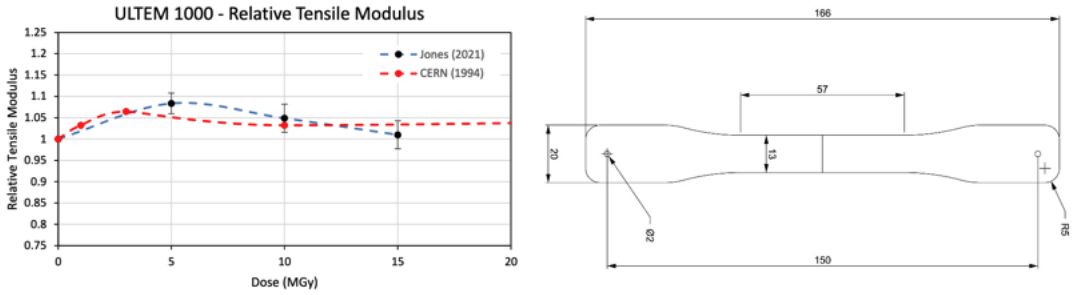


**Figure 13:** Left: results of the tensile modulus measurement relative to the nominal value (unirradiated sample) where only variations below 10% are observed after irradiation, each value correspond to the average of three samples. Right: diagram of a dogbone sample.

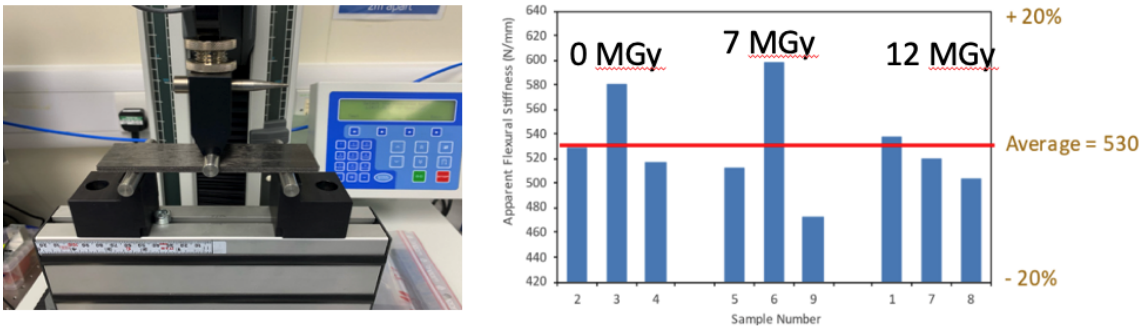


**Figure 14:** Three point bending test. Left: picture of one sample undergoing the test. Right: results for un-irradiated samples, and samples irradiated up to 7 and 12 MGy (3 samples of each).

pre-production stage and expects to start production in mid 2023. Both subsystems have already produced and qualified a few pre-production objects. The Inner System is about to start pre-production and expects to be ready for production in early 2024.

## 5. Acknowledgements

This work could never have been presented without the tireless work of the ITk-Pixel community. In this case, special recognition goes to the local support teams of the three subsystems: Outer Barrel, Outer Endcaps and Inner System.

## References

[1] High Luminosity LHC project, https://hilumilhc.web.cern.ch/.

[2] ATLAS Collaboration, Technical Design Report for the ATLAS Inner Tracker Strip Detector, CERN-LHCC-2017-005, 2017.

[3] ATLAS Collaboration, Technical Design Report for the ATLAS Inner Tracker Pixel Detector, CERN-LHCC-2017-021, 2017.

[4] ATLAS Collaboration, Expected tracking and related performance with the updated ATLAS Inner Tracker layout at the High-Luminosity LHC, ATL-PHYS-PUB-2021-024, 2021.

[5] M. Tavalet (CERN) and H. van der Burgt (ERTA-EPEC), Radiation resistance and other safety aspects of high-performance plastics by ERTA, presented at "Workshop on Advanced Materials for High-Precision Detectors", September 1994. CDS link